THE OHIO STATE UNIVERSITY

TARGET SIGNATURE MODELING AND BISTATIC SCATTERING MEASUREMENT STUDIES

W. D. Burnside, T. H. Lee, R. Rojas
R. J. Marhefka, D. Bensman

The Ohio State University

ElectroScience Laboratory

Department of Electrical Engineering
Columbus, Ohio 43212

Annual Report
721432-2, 721446-2, 721447-2, and 721711-3
Grant No. NAG2-542
September 1988 – August 1989

NASA - Ames Research Center
Moffett Field, CA 94035

NOTICES

When Government drawings, specifications, or other data are used for any purpose other than in connection with a definitely related Government procurement operation, the United States Government thereby incurs no responsibility nor any obligation whatsoever, and the fact that the Government may have formulated, furnished, or in any way supplied the said drawings, specifications, or other data, is not to be regarded by implication or otherwise as in any manner licensing the holder or any other person or corporation, or conveying any rights or permission to manufacture, use, or sell any patented invention that may in any way be related thereto.

50272-101

REPORT DOCUMENTATION PAGE	1. REPORT NO.	2.	3. Recipient's Accession No.

4. Title and Subtitle
Target Signature Modeling and
Bistatic Scattering Measurement Studies

5. Report Date
Sept. 1988 – Aug. 1989

6.

7. Author(s) W. D. Burnside, T. H. Lee, R. Rojas
R. J. Marhefka, D. Bensman

8. Performing Org. Rept. No.
721432-2, 721446-2, 721447-2, 721711-3

9. Performing Organization Name and Address
The Ohio State University
ElectroScience Laboratory
1320 Kinnear Road
Columbus, OH 43212

10. Project/Task/Work Unit No.

11. Contract(C) or Grant(G) No.
(C)
(G) NAG2-542

12. Sponsoring Organization Name and Address
University Affairs Branch, NASA - Ames Research Center
M/S 241-25
Moffett Field, CA 94035

13. Report Type/Period Covered
Annual Report

14.

15. Supplementary Notes

16. Abstract (Limit: 200 words)

This is an annual report that summarizes the work done on Grant No. NAG2-542 during the period 1 September 1988 to 31 August 1989. There are four areas of study to be summarized: 1) Bistatic scattering measurement studies for a compact range. 2) Target signature modeling for test and evaluation hardware in the loop situations. 3) Aircraft code modification study. 4) SATCOM antenna studies on aircraft.

17. Document Analysis a. Descriptors

Measuements
Modelling
Scattering
Diffraction
Bistatic
Imaging

b. Identifiers/Open-Ended Terms

c. COSATI Field/Group

18. Availability Statement
A. Approved for public release;
Distribution is unlimited.

19. Security Class (This Report)
Unclassified

21. No. of Pages
48

20. Security Class (This Page)
Unclassified

22. Price

(See ANSI-Z39.18) *See Instructions on Reverse* OPTIONAL FORM 272 (4-77)
Department of Commerce

Blank Page

Contents

List of Figures

Chapter 1

Introduction

This is an annual report that summarizes the work done on Grant No. NAG2-542 during the period 1 September 1988 to 31 August 1989. There are four areas of study to be summarized:

1. Bistatic scattering measurement studies for a compact range. This work is being conducted by T. H. Lee and W. D. Burnside under Ohio State University project number 721432.

2. Target signature modeling for test and evaluation hardware in the loop situations. This work is being conducted by R. J. Marhefka under Ohio State University project number 721446.

3. Aircraft and missile code modification studies. This work is being conducted by R. Rojas under Ohio State University project number 721447.

4. SATCOM antenna studies on aircraft. This work is being conducted by R. J. Marhefka and D. Bensman under Ohio State University project number 721711.

   An overview of the research accomplished is described in the separate chapters below.

Chapter 2

Bistatic Measurement Study

This is a summary of the portion of the grant pertaining to bistatic measurement study.

2.1 Introduction

The goal of this project is to study bistatic scattering measurement in the compact range and techniques of image processing of bistatic scattered fields to obtain the bistatic scattering centers. The determination of scattering centers is very important in diagnostic radar application in that one can accurately distinguish various dominant scattering terms associated with specific features on a target based on its scattering characteristics. Under this study, two image processing techniques which use the bistatic scattered fields of the target to determine the scattering centers of the target have been developed. In general, the transmitting and receiving antennas for the bistatic scattering measurement can be either two compact ranges or one compact range and a horn antenna. The compact range reflector can be either focussed or defocussed so that a near-field situation can be simulated. As a special case, when two identical compact range reflectors are co-located to do a bistatic scattering measurement, one has a backscatter measurement. Consequently, the same techniques can be used to determine the backscatter scattering centers. Bistatic

scattering measurements of several spheres has been performed in OSU compact range. The bistatic scattered fields were collected as a function of frequency and angle of incidence. Then, cross-range and down-range images of the target are determined. The image processing techniques are summarized next.

2.2 Focussed Image Processing Technique

A focussed image processing technique has been developed and reported in [1,2]. In a conventional image processing technique, a Fast Fourier Transform is applied to the backscattered fields of a target to determine the scattering centers. This requires that the antenna be located in the far field of the target and that the target be rotated only through small angles. This assumption is not true in general because there are many situations for which the antenna is in the near zone of the target. Consequently, a more general image processing technique has to be used.

The focussed image processing technique is a more general approach to determine the scattering centers of the target, either from the backscattered fields or the bistatic scattered fields. The key factor associated with focussed image processing techniques is the knowledge of the phase history of the scattering centers associated with a given illumination. The scattered fields, which are normally collected as functions of frequency and angle of incidence, are processed by multiplying the received response by a phase factor which is complex conjugate of the phase associated with the path length from the source to the potential scattering center and then to the receiver. For a given scattering center location, the various responses are summed over the frequency band and the region of angular rotation. As a result, the summed responses at a true scattering center is more enhanced than those which are not true scattering centers.

The detail of this technique and the images obtained from measurement of several targets can be found in [1,2]. One disadvantage of this general focussed image processing technique is the large amount of computation time required for processing. A more efficient ap-

proach which uses the time domain response of the target has also been developed and will be discussed next.

2.3 Image Processing Using Time Domain Data

In general, one normally measures both the angular domain and frequency domain data associated with the target. A reference target, such as a sphere, is also measured. Then the measured scattered fields of the target are calibrated with respect to the reference sphere so that the scattering cross section of the target as a function of frequency and target angle of rotation is determined. When these calibrated scattered fields are processed by a general focussed image processing technique, the scattering centers associated with the target are determined with respect to the location of the center of the reference sphere. As discussed in the previous section, the summation over frequency domain and angular domain is a very time consuming effort. However, it is well known that the frequency domain data can be Fourier transformed into time domain data via a very efficient approach known as Fast Fourier Transform. As a result, the time domain data can also be used to determine the cross-range and down-range images of the target. The general approach of using time domain data for image processing is discussed in this section.

The time domain data obtained for a given angle of target rotation contains information related to the location of scattering centers relative to the reference target along the axis of illumination. A given point on the time axis represents the time required for a wave to travel from the source to a point in the image plane and then to the receiver as referenced to the time of travel from source to the reference target and then to the receiver. For a given set of time domain data, one can fill the time domain response over the whole image plane. As a result, one obtains lines of response in the image plane in that each line represents the locus of equal distance from the source through the target and to the receiver. For example, if two focussed compact ranges are used in the measurement, the locus of equal distance is

a straight line. If one uses a focussed compact range reflector with another horn antenna located in the near field of the target; i.e., the horn antenna has a spherical wave illumination, the locus of equal distance is a parabola. The time domain response amplitude represents the scattering level of the target. The amplitude of the response is the same along the locus of equal distance. Note that the amplitude of the response function associated with a true target scattering center is more significant than the others. For a given time domain data, one will obtain a line of scattering centers in the image plane in that the down-range location of the scattering center can be easily identified; while, the cross-range image can not be determined because of very poor resolution. However, if the time domain responses associated with different angles of incidence are processed, the resulting image will appear to emphasis the true scattering centers which will appear as peak values. In other words, the peak time domain responses for different angles of rotation will intersect to each other at the scattering center such that not only the down-range but also the cross-range images of the target can be identified. This is true when more than one scattering center is present. Although the scattering centers can be identified by just using time domain data for two angles of rotation, one needs more data in order to improve the resolution of the images. This can be achieved by summing time domain responses for a region of target rotation angles. If a true scattering center exists, the overall response will be a peak at the scattering center location as compared to other locations.

There are two advantages of this time domain approach. First, the computation time is much more efficient than the focussed image processing technique because the frequency domain data can be Fast Fourier transformed to the time domain while in the focussed processing technique, the frequency domain data has to be summed which takes more computation time to do. Secondly, one can do real time imaging by using time domain data. In conventional focussed imaging technique, one has to collect all the frequency domain data for all of the target rotation angles before the processing can be started. On the other hand, the frequency domain data associated with one angle of rotation can be processed once it is collected. Then, the resulting time domain data can immediately be summed with previous

results to form the image of the target. This image can then be displayed. Note that as a new set of frequency data is obtained, it can be processed and then added to the previous image to obtain a new image with a better resolution. As a result, one can observe the image as it evolves. Once all the measurements are finished, the image of the target is obtained. Both of these two advantages make the real time image processing technique more useful than the conventional focussed imaging approach.

2.4 Summary

Two methods of image processing techniques using the measured backscattered or bistatic scattered fields obtained in a compact range have been developed under this project. Both methods have been found to be able to accurately determine various scattering centers of a target through measurements. In addition, the time domain imaging approach is very time efficient and can be used to display scattering centers in a real time basis. These image processing techniques will be very useful in diagnostic radar application for both backscatter and bistatic scatter cases.

Chapter 3

Target Signature Study

This is a brief review of the portion of the grant pertaining to target signature modeling.

3.1 Introduction

The objective of this part is to determine and implement an effective method to integrate the use of UTD electromagnetic prediction codes for simulation of radar cross section into test and evaluation situations. UTD scattering code predictions can replace costly measurements. The signatures are used in the test loops to evaluate how effectively radar can follow targets. In this situation, it is necessary that the data be efficiently obtainable.

3.2 Scattering Code Overview

The use of the UTD based code RCS - Basic Scattering Code [3] is being evaluated for test and evaluation purposes. It explicitly defines the specular, edge, and vertex diffraction points, as well as many higher order terms. It uses efficient ray tracing techniques based on the chosen geometry models. It does not need integration of currents

since it uses closed form diffraction coefficients. This allows the flexibility to store the characteristics of specific scattering centers of a target and then add the field information versus angle or frequency as they are needed. Since test and evaluation hardware in the loop situations need efficiency and flexibility of operation, this type of approach will be beneficial for large sized targets and the many angles of approach needed. In addition, it has a bistatic scattering capability that might be useful in the future.

A study of the various UTD mechanisms that will be most important for modeling in the test and evaluation situation has been undertaken. Their theoretical characteristics have been studied from the point of view of obtaining the best way to determine, calculate and store each term individually [2]. The UTD radar cross section prediction code, RCS-BSC version 2, has been modified so that its write algorithms for the UTD mechanisms calculated will better accommodate a volumetric output of the individual fields.

The RCS-BSC version 2 corner diffracted field section as been modified to allow access of an individual corner diffracted field instead of an edge in order to study which is the best way to store the fields in the data base. Other field sections will be modified as they are integrated into the data base. The particular terms needed are being determined based on the comparing the code with measurements of various scale models of aircraft as discussed in the next section.

3.3 Code Evaluation

Test cases, that will represent meaningful situations for test and evaluation purposes, are being used to validate the algorithms being developed. A model of a QF-100 aircraft has been suggested by K. Oh and C. L Yu at Pacific Missile Test Center, since they have measured data on a one fourth scale model. The geometry is illustrated in Figure 3.1. The geometry used in the computer code is illustrated in Figure 3.2.

The backscattered measured pattern in the azimuth plane for horizontal polarization at 10 GHz is shown in Figure 3.3. The far zone

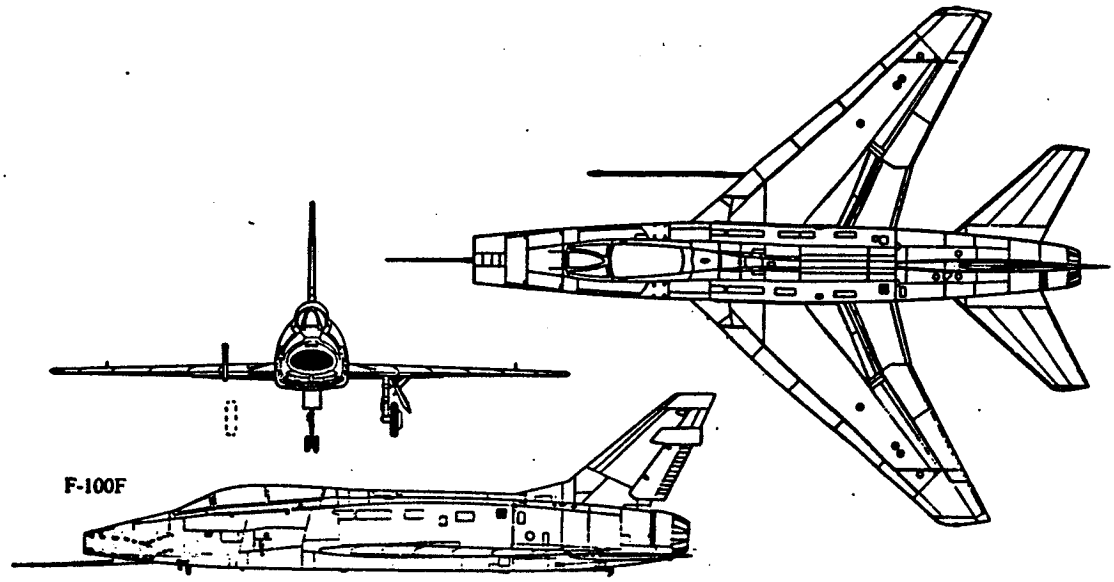

Figure 3.1: Drawing of a QF-100 aircraft (*Jane's* 1961-62).

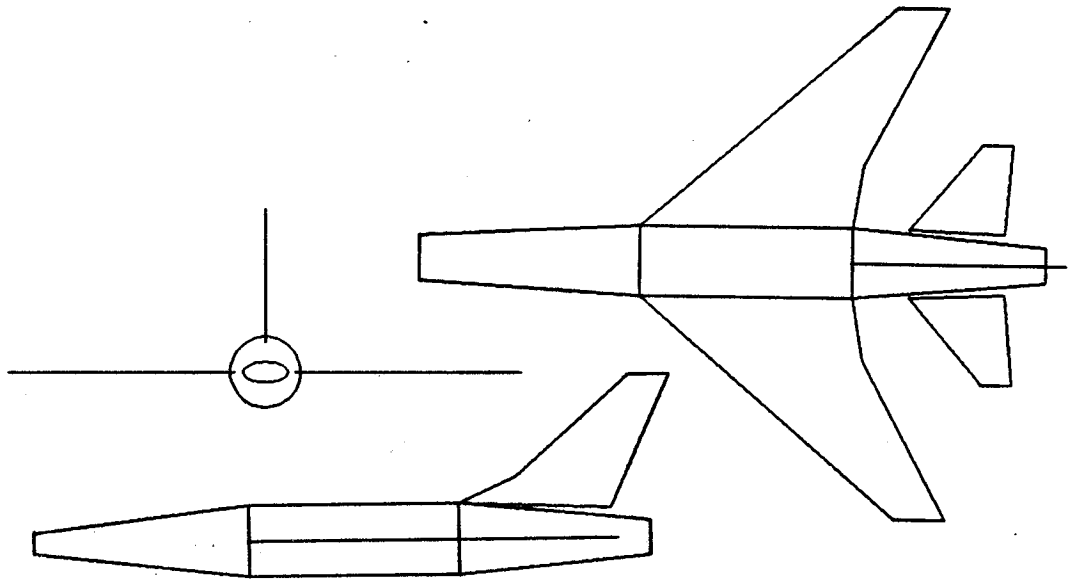

Figure 3.2: Geometry used to computer model a QF-100 aircraft.

calculated result [3] is shown in Figure 3.4. The measurements have been taken on the spherical range at PMTC at a distance of approximately 72 ft. In order to illustrate the near zone effects of the range [4], the result for just the fuselage (cone frustum) calculated at the 72 distance is shown in Figure 3.5. Note that the broadening effect of the lobes at $\pm 90°$ is clearly visible. The backscattered measured pattern in the azimuth plane for vertical polarization at 10 GHz is shown in Figure 3.6. The far zone calculated result is shown in Figure 3.7. Notice that for both polarizations the peaks associated with the fuselage and wing edge speculars are in the general area of the measurement peaks. Obviously, there is a lot more scattering from the model than is accounted for in the calculations. The main contributors are most likely the fact that the real model has a engine duct present, whereas, the computer model has a flat plate. Also, the real model has an extensive cockpit configuration which is not model at all by the computer model.

More measured and calculated model will be compared in the future. Cleaner models should show better agreement. Computer modeling can be shown to be quite accurate for many scattering features. As the QF-100 comparisons show, however, real aircraft have quite a few addition scattering features that are not always easy to model with the present state of the art. Possible ways to supplement the computer models will be investigated in the future.

3.4 Further Work

Computer codes can be used to accurately and efficiently predict the scattering of many of the features of real aircraft. However, real aircraft have many addition scattering centers or physical phenomenon for which diffraction coefficients are not available or the situation is too complex to model for large sized structures. The alternative is to combine calculations and measurements in a single data base. The most efficient and/or accurate method will be used when warranted. A three dimensional imaging technique with corresponding data base is recommended. This will be investigated in the coming year.

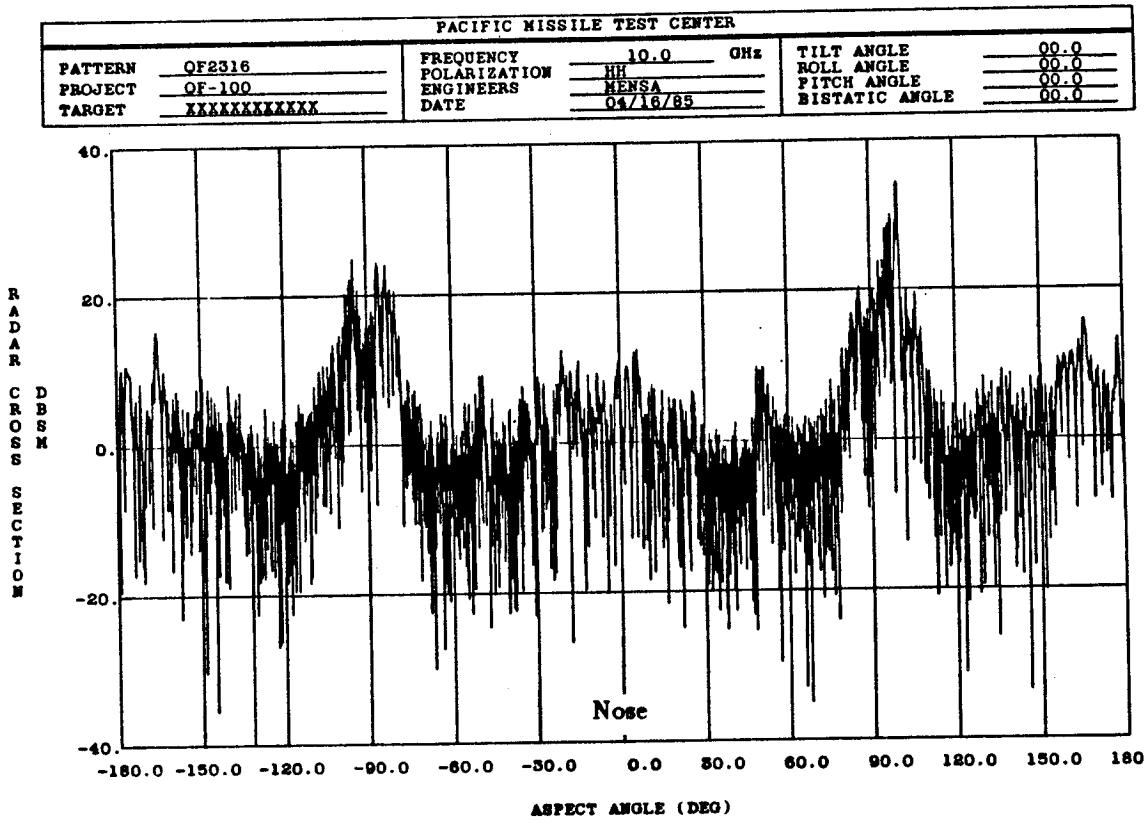

Figure 3.3: Backscatter from a model of a QF-100 for horizontal polarization at 10 GHz in the azimuth plane measured at PMTC.

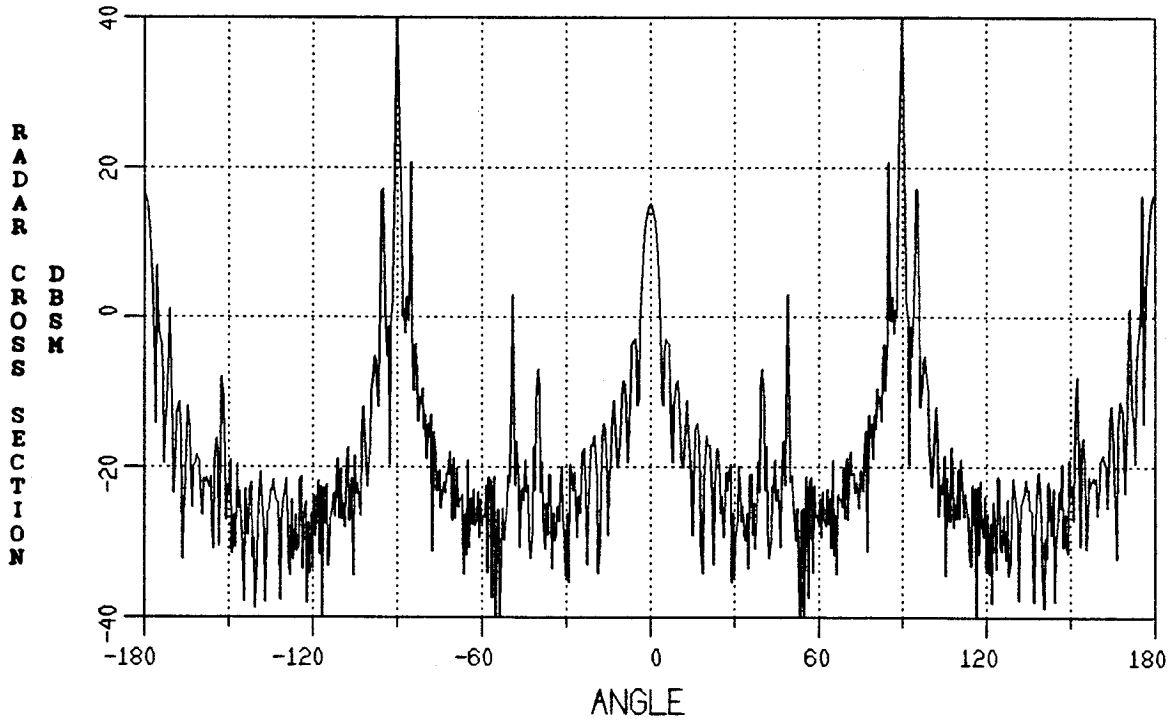

Figure 3.4: Backscatter for a model of a QF-100 for horizontal polarization at 10 GHz in the azimuth plane calculated using RCS-BSC.

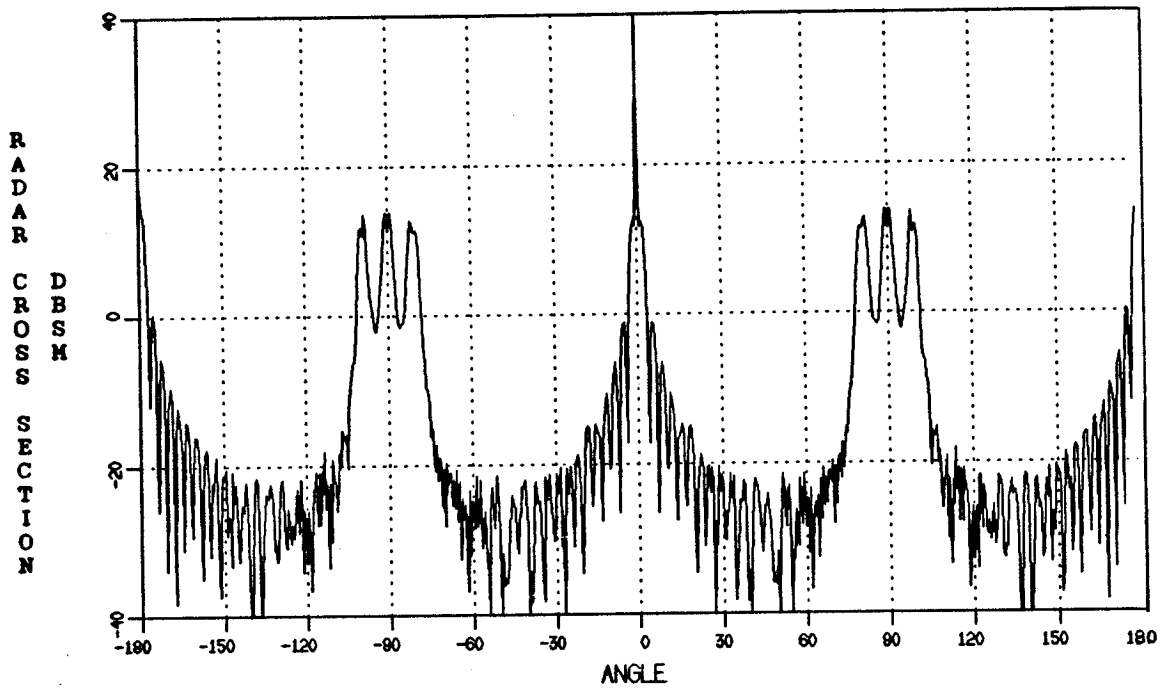

Figure 3.5: Backscatter for a model of the fuselage only of a QF-100 for horizontal polarization at 10 GHz in the azimuth plane calculated at 72 ft distance using NEC-BSC.

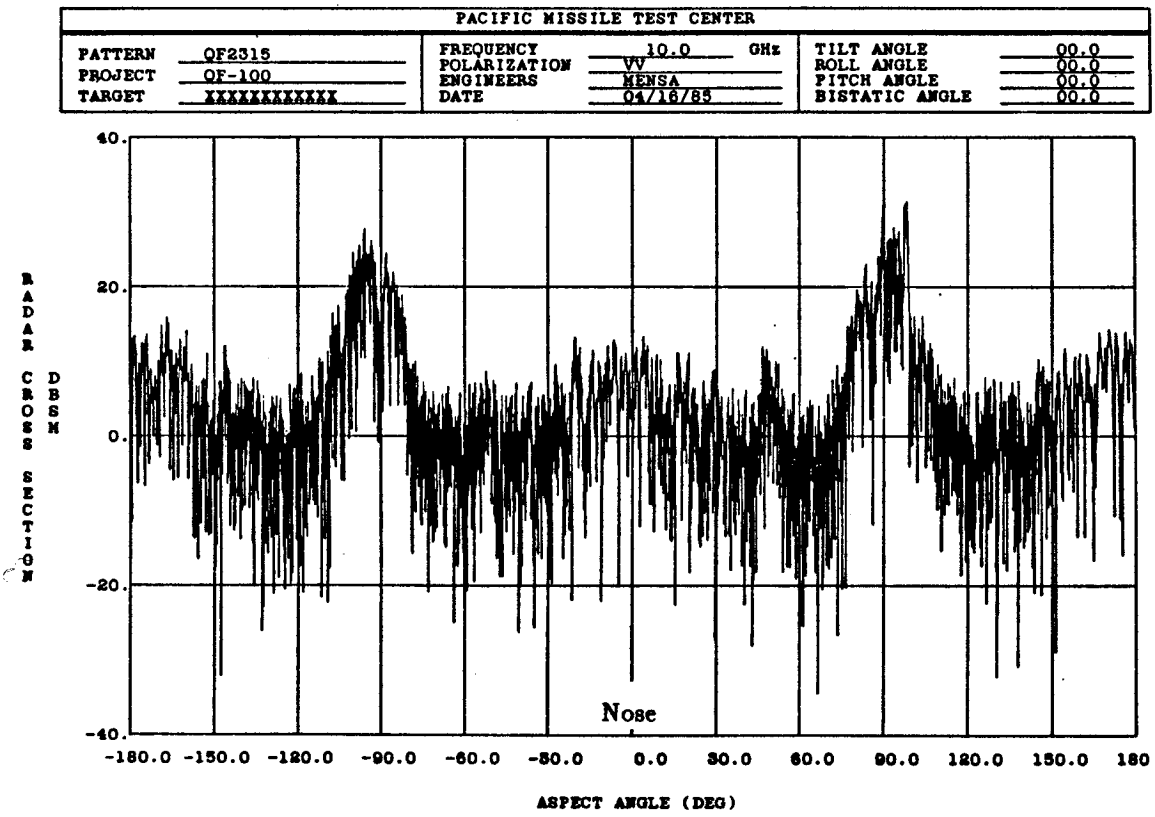

Figure 3.6: Backscatter from a model of a QF-100 for vertical polarization at 10 GHz in the azimuth plane measured at PMTC.

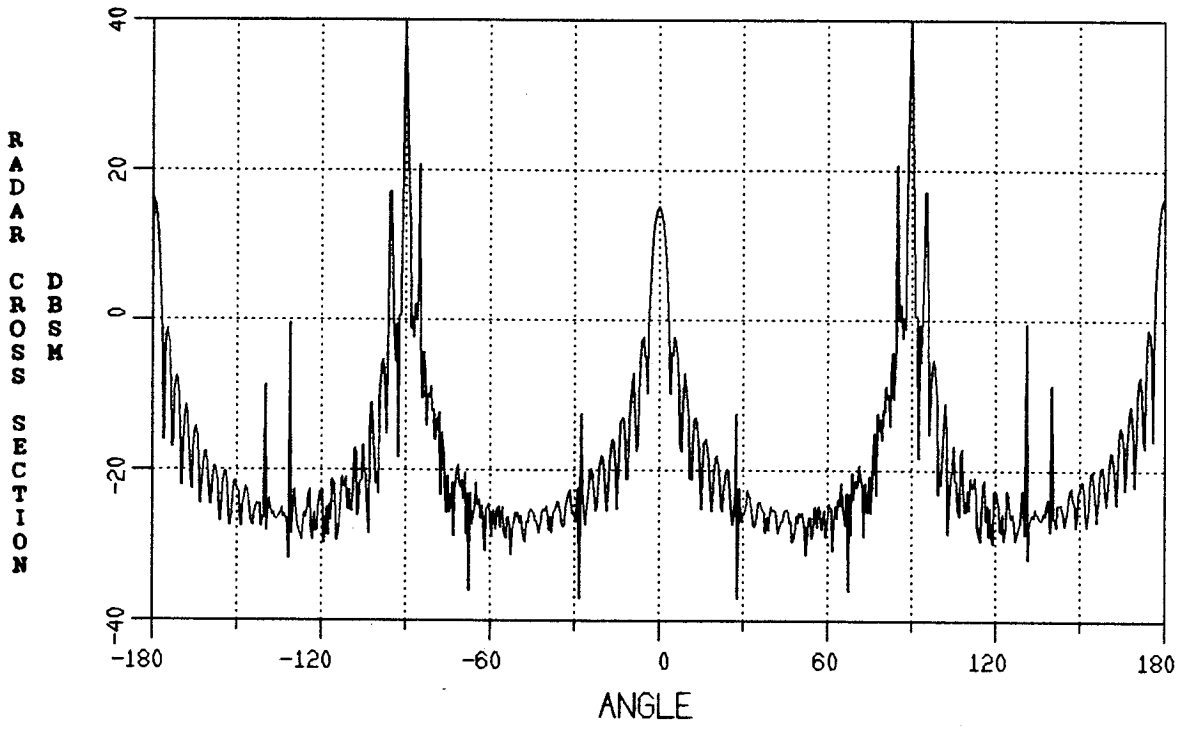

Figure 3.7: Backscatter for a model of a QF-100 for vertical polarization at 10 GHz in the azimuth plane calculated using RCS-BSC.

Chapter 4

Aircraft Code Study

4.1 Introduction

In this chapter, the modification of the well known NEWAIR3 code, also known as the aircraft and missile antenna code [5], is discussed. The two most important modifications are:

(a) A smoothing algorithm has been added to the NEWAIR3 code. This algorithm smooths the output data generated by running the code. This capability is useful when the output data contains spikes and jumps due to numerical problems.

(b) The code has been modified to include the radiation by a rectangular microstrip patch. The rectangular microstrip patch is shown in Figure 4.1.

(c) This code, originally written for a mainframe computer such as the VAX 8550, has been modified so it can be run on a personal computer.

The aircraft and missile antenna code [5], which is written in standard Fortran 77, has been developed at The Ohio State University to investigate the radiation patterns of antennas mounted on an aircraft or missile fuselage which is modelled by a composite ellipsoid. This code was originally developed by Prof. Burnside and the present

code (NEWAIR3) is the third version. This computer code is used to compute the near and far zone radiated fields for antennas mounted on a composite ellipsoid and in the presence of a set of flat plates. Since the NEWAIR3 code is based on the uniform geometrical theory of diffraction (UTD), the structures that can be analyzed have to be electrically large. In terms of the scattering from plate structures, this means that each plate should have edges at least a wavelength long. In terms of the composite ellipsoid structure, its major and minor radii should be at least a wavelength in extent. In addition, each antenna element should be at least a wavelength from all edges. In some cases, the wavelength limit can be reduced to a quarter of wavelength for engineering purposes.

The code allows the user to simulate a wide variety of complex electromagnetic radiation problems using the ellipsoid/plates model. For example, the composite ellipsoid can be used to accurately simulate the fuselage of an aircraft or missile; whereas, the plates are used to represent the wings, stabilizers, stores, engines, etc. This code can also be used to simulate the radiation of an antenna mounted directly on a ship mast. In this case the mast can be modelled by the composite ellipsoid with the other ship structures simulated by the flat plates. Note that the plates can be attached to the composite ellipsoid and/or to other plates. In fact the plates can be connected together to form a box. Although this code can be used to simulate a wide variety of complex structures, it is specifically designed to analyze the radiation characteristics of antennas mounted on aircraft configurations.

The NEWAIR3 code has the flexibility to handle arbitrary pattern cuts in the near or far field regions. All the components of the radiated electric field are computed but only the fields E_ϕ and E_θ are stored in a binary file for later use; however, the code can be easily modified such that the user can store additional field components.

This code has a user's manual [5] which is designed to give an overall view of the operation of the computer code, to instruct the user in how to use it to model structures, and to show the validity of the code by comparing various computed results against measured data whenever available. The present code requires approximately 707K

bytes of storage (VAX 11/780). It will run a pattern cut of 360 points for a commercial aircraft model with one antenna element in approximately 4 minutes in a VAX 11/780 computer.

4.2 Smoothing Algorithm

The existing Ohio State University Aircraft code (NEWAIR3) has been modified so that any spikes in the radiation patterns are removed by a smoothing algorithm. The input data for the EX: command [5] has been modified as follows:

EX:
LSMOOTH, NAVG, SEN

where

LSMOOTH = T, spikes are removed from the output data
F, the output data is not modified

NAVG = # of data points used to compute an average.
It is always even, usually NAVG=4.

SEN = # of standard deviations that is allowed before a spike is removed. SEN does not have to be an integer.

Note that when LSMOOTH=F, the code does not use the parameters NAVG and SEN; however, they still have to be enter.

4.3 Microstrip Path antenna

The NEWAIR3 code can handle an arbitrary antenna type provided the current distribution across the aperture is known. This is done by

approximating the distribution by a set of magnetic current elements mounted on or electric current elements normal to the composite ellipsoid surface. The magnetic current elements have a cosine distribution along the magnetic current direction and a uniform distribution in the orthogonal direction. The normal electric current represents a monopole and its length can not be greater than a quarter wavelength.

In order to model a rectangular microstrip patch, a very well known and simple cavity [6] model can be used to represent this type of antenna as depicted in Figure 4.2. That is, if one assumes that the antenna is operating at or near the lowest order resonant frequency TM_{10}, namely

$$f_{10} = \frac{c}{2b\sqrt{\epsilon_r}} = \frac{1}{2b\sqrt{\epsilon\mu_o}} \; ; \; \epsilon_r = \frac{\epsilon}{\epsilon_o}$$

where c and μ_o are the speed of light and the permeability in free-space, respectively, and ϵ is the permittivity in the substrate. The microstrip patch can then be replaced by two magnetic dipoles as shown in Figure 4.2. The current is constant along the length of the dipole and it is given by

$$\vec{I}_m = -\hat{y}C_{10}t \; ; \; \begin{array}{ll} x = -a/2, & -b/2 \le y \le b/2 \\ x = \; a/2, & -b/2 \le y \le b/2 \end{array} \tag{4.1}$$

where t is the thickness of the substrate and

$$C_{10} = \frac{-2jk_o\eta_o I_o \sin\left(\frac{\pi x_a}{b}\right)}{(k_o^2\epsilon_r - k_{10}^2)ab} \tag{4.2}$$

In (4.2), k_o, η_o, ϵ_r, and I_o are the free-space wave number, the intrinsic impedance of free space, the relative permittivity and the current at the feed point (x_o, y_o), respectively. The wavenumber k_{10} is given by

$$k_{10} = \frac{\pi}{b}.$$

Since the aircraft code already models a magnetic dipole by a slot [5,7], we can also replace the two magnetic dipoles in (4.1) by two slots. However, there is one important difference with the model that already exists in the code. In the aircraft code, the fields in the slot

have a cosine distribution along the long dimension of the slot. The current in (4.1) is constant and therefore the field description along the long dimension of the slot replacing this dipole has to be constant.

The NEWAIR3 code has been modified in such a way that it can now calculate the radiation of a single rectangular microstrip patch. The input command SG:, which is described in the user's manual [5] has been modified as follows:

```
SG:
PHS, ZS
MSX
RHOA(MS), PHIA(MS)
SLOTAA(MS), SLOTBB(MS), BETADA(MS), SMONOA(MS), JANTA(MS)
WMA(MS), WPA(MS)
TSE, XO, YO, CER,CERI
```

The parameter JANTA(MS), which defines the type of antenna, has been modified as follows:

$$\text{JANTA(MS)} = \begin{cases} 1, & \text{SLOT ANTENNA} \\ 3, & \text{RADIAL MONOPOLE ANTENNA} \\ 2, & \text{MICROSTRIP PATCH ANTENNA} \end{cases}$$

Note that for the microstrip patch $MSX = 1$; whereas, for the other two cases $1 \leq MSX \leq 10$.

When JANTA(MS)=1 or 3, all the parameters of the SG: command are as before [5], except that the last line, namely, TSE, X0, Y0, CER, CERI should not be input. On the other hand, when JANTA(MS)=2, the parameters PHS, ZS, RHOA, PHIA are the same, but SLOTAA and SLOTBB are the short and long dimensions, respectively, of the the microstrip patch antenna as depicted in Figure 4.3. Furthermore, $BETADA$ is the angle between the axis of the fuselage and the microstrip antenna as shown in Figure 4.3, TSE is the thickness of the substrate, $(X0, Y0)$ are the coordinates of the feed point and CER and $CERI$ are the real and imaginary parts of the relative dielectric constant.

For purposes of illustration, a simple case is considered here to test the validity of the model used to simulate the microstrip patch. An input

data set is depicted in Figure 4.4 for a circumferential rectangular patch mounted on a composite ellipsoid. The far field roll plane cut is shown in Figure 4.5. This result is a reasonable approximation of the radiation pattern of a microstrip patch.

4.4 PC version of Aircraft code

The Aircraft code has also been implemented on a personal computer. In order to accomplish this task, additional memory and software were obtained for a IBM AT compatible computer. The FORTRAN compiler that was obtained is a Microway NDP FORTRAN-386 compiler. Note that to run the code, it is necessary to have 4 Mbytes of memory.

The Aircraft code had to be modified in certain places in order to compile it in the personal computer. However, for the most part, the changes were minor.

This modified code was used to run the case considered in Figure 4.4. As expected, exactly the same result as in Figure 4.5 was obtained. Another case was also run which is similar to Example 2 in the user' manual [5]. The input data is shown in Figure 4.6 and the geometry is the same as in Figure 13 of the user's manual. That is, this case considers the radiation by a short monopole mounted on a composite ellipsoid with a wedge attached to the fuselage. The calculated pattern (in the roll plane) is depicted in Figure 4.7 for the E_ϕ field component. The pattern calculated by the NEWAIR3 code in the VAX computer is also included to make sure that the modifications in the PC version are correct.

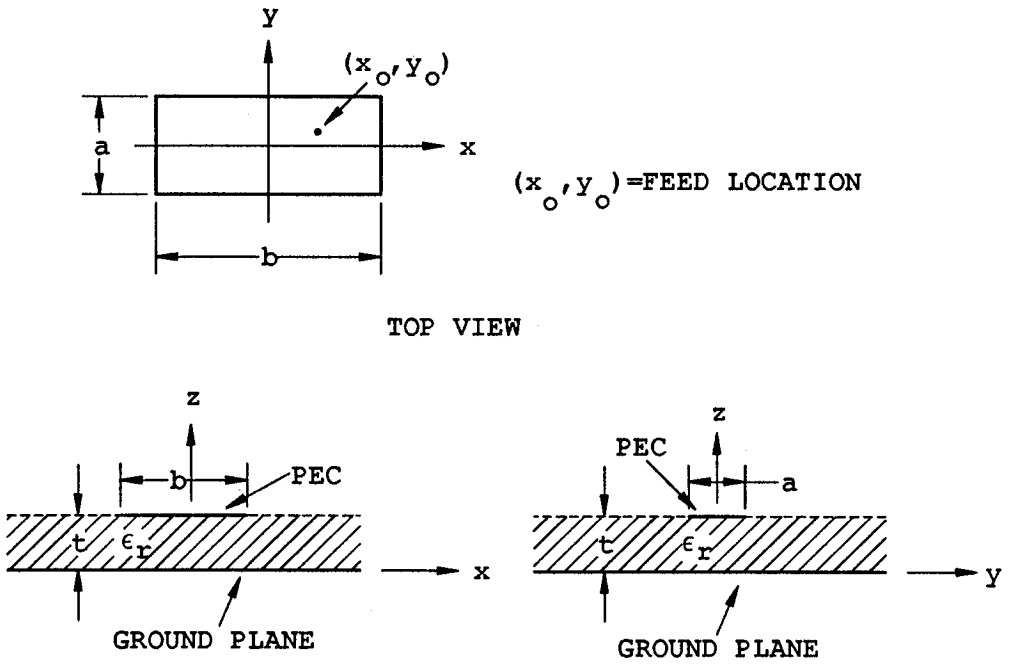

Figure 4.1: Rectangular microstrip antenna.

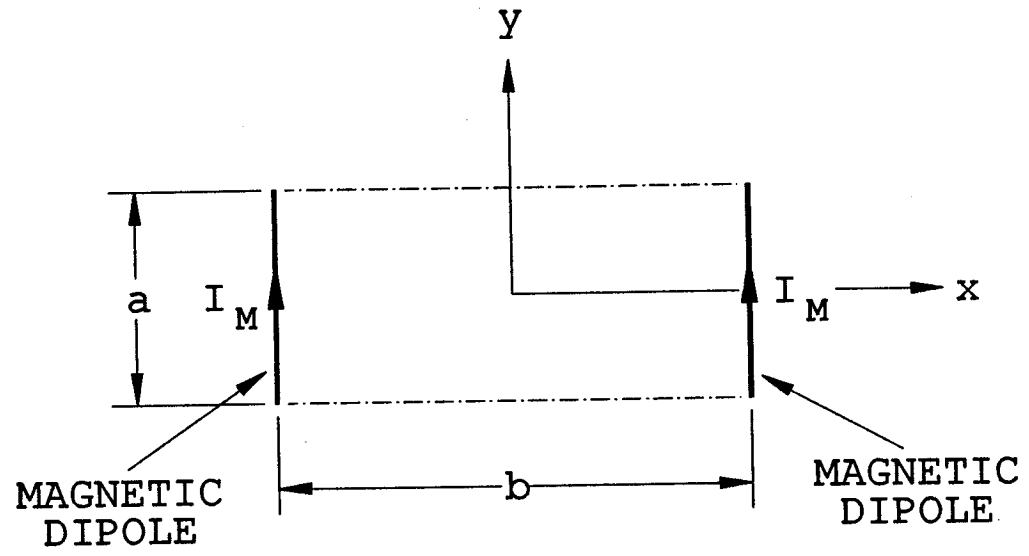

Figure 4.2: Cavity model for rectangular microstrip antenna operating near the lowest order resonant frequency f_{10}.

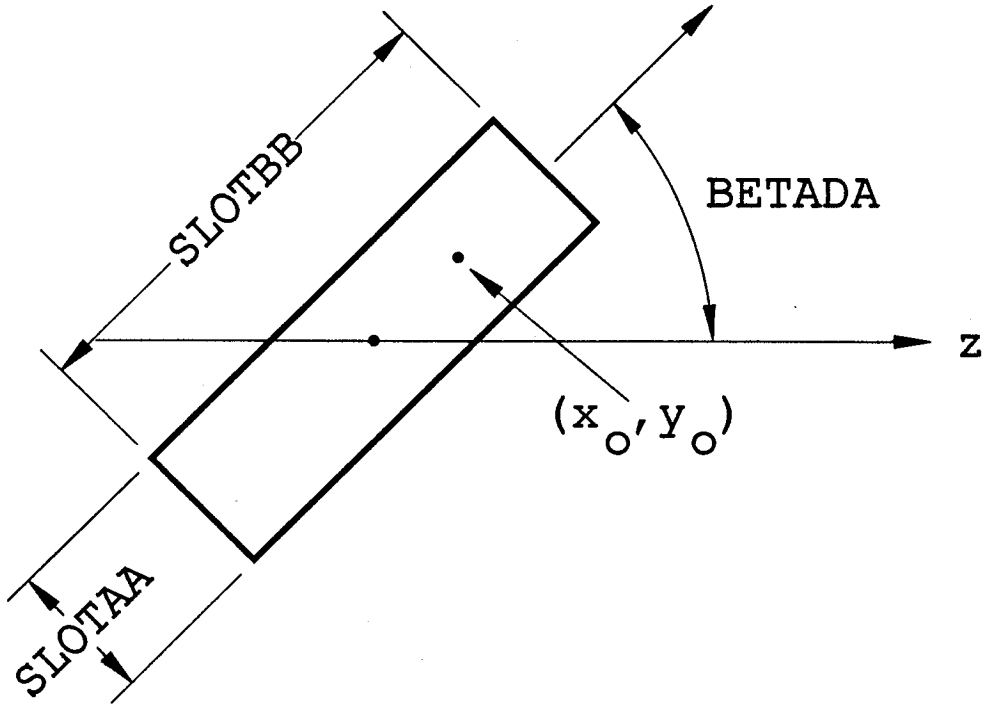

Figure 4.3: Definition of dimensions SLOTAA and SLOTBB and angle BETADA

```
UN: INCHES
3
FQ: 3. GHZ
1,3.,1.
FG:
25,30,150,80
F
0,0,0
SG:MICROSTRIP PATCH
0.,0.01
1
0,0
.5,1.,90.0,.25,2
1,0
0.05,0.1,0.,4.,0.
PD: ROLL PLANE
0,0,90
0,360,1
T,1000
BO:
T
EX:
F,4,2.
```

Figure 4.4: Input data to calculate radiation by a single microstrip patch.

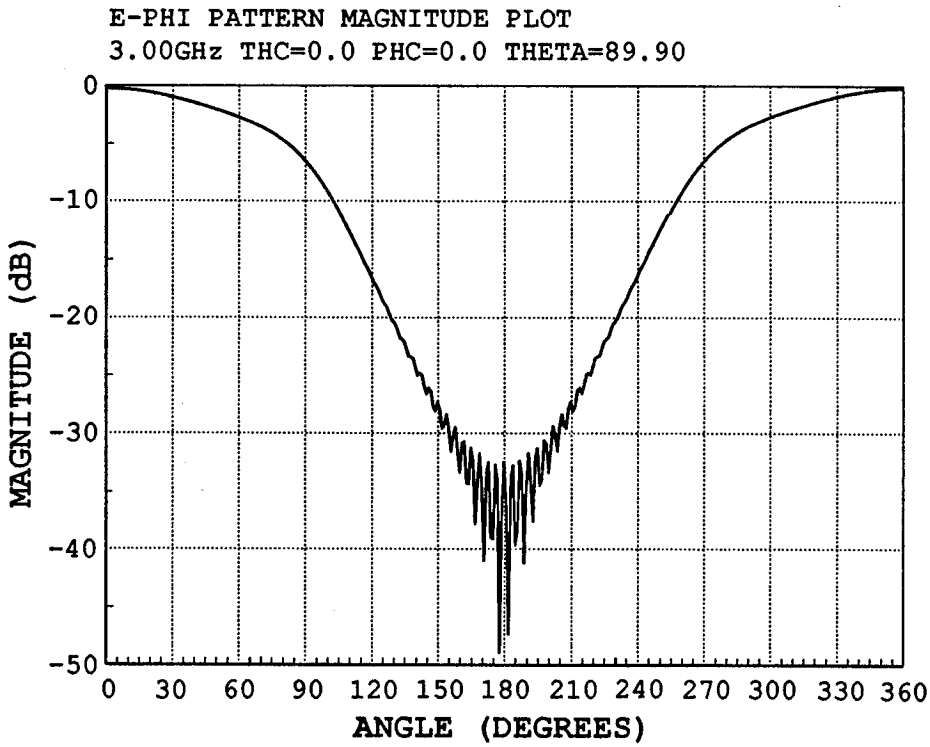

Figure 4.5: Radiation pattern of rectangular microstrip patch antenna.

```
UN: FEET
2
FQ: 1. GHZ
1,1.,1.
FG:
5.,6.,50.,50.
F
0,0,0
FB:
2
4
4.5,0.,20.
4.5,0.,-20.
-4.5,0.,-20.
-4.5,0.,20.
4
0.,-5.5,20.
0.,5.5,20.
0.,5.5,-20.
0.,-5.5,-20.
SG: MONOPOLE
0.,0.
1
0.,0.
0.4,0.8,0.,0.25,3
1.,0.
BO:
T
PD: ROLL PLANE
0,0,90
0,360,1
F,1000
PG:
4,T
3.,6.,-20.
3.,9.,-20.
3.,9.,20.
3.,6.,20.
PG:
4,F
3.,9.,-20.
10.,18.,-20.
10.,18,20.
3.,9.,20.
EX:
F,4,2.
```

Figure 4.6: Input data for monopole mounted on a composite ellipsoid. This data set was run on the PC version of the NEWAIR3 code.

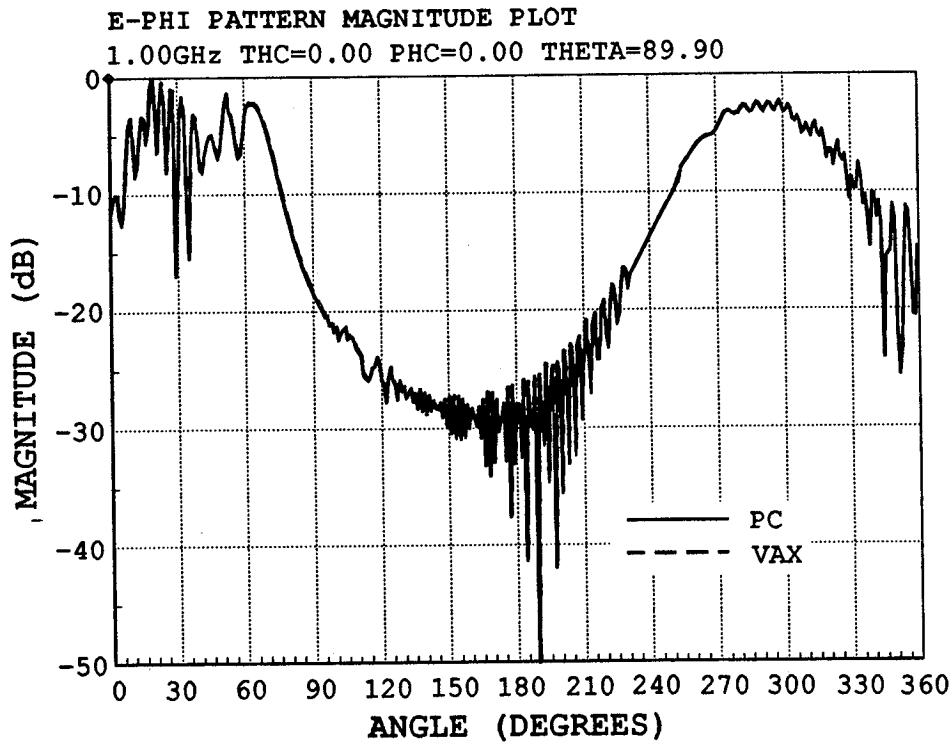

Figure 4.7: Radiation pattern of a monopole mounted on a composite ellipsoid as shown in Figure 13 of [5]. The input data is shown in Figure 4.6.

Chapter 5

SATCOM Antenna Study

This is a brief review of the portion of the grant pertaining to satellite communication antenna (SATCOM) modeling. The summary described here is to be presented at the ACES meeting in March 1990 entitled "A SATCOM Antenna Siting Study on an Aircraft Using the NEC-BSC V3.1" by R. J. Marhefka, D. Bensman, and D. DeCarlo.

5.1 Introduction

This paper discusses the use of the NEC - Basic Scattering Code Version 3.1 (NEC-BSC31) to predict the patterns of a UHF SATCOM antenna on an aircraft. The ultimate objective is to find a location or locations of the antenna to maintain the satellite link in areas of high signal fading to multipath effects. In this case, the antenna is a commercially available circularly polarized crossed dipole type system. The aircraft is a P-3C.

The use of a code, such as the NEC-BSC31, in studies like this can ease costs by reducing though not eliminating measurements. Many locations can be tried in a reasonably fast time. Measurements are still needed, however, to validate the code. This paper concentrates on the model set up and the validation steps. First, setting up the code to present the circular polarization normalized to circular isotropic is discussed. Next, how the antenna is modeled is presented. The

methodology of defining the aircraft model is next discussed. Finally, the validation of the model is presented.

5.2 Background

The analysis is performed using the NEC - Basic Scattering Code Version 3.1 [4]. The complete capabilities of this code are detailed in the manual and have been summarized in previous papers [8]. The theory, based on UTD, has also been discussed in many references [9,10]. The main discussion here is centered around using the code to define a particular type of model and validation of the model.

In defining a model, it is necessary to compare the needs of the applications with the limitations of the available capabilities of the code. Some of the missing elements can be added. Others will have to be circumvented by careful definitions of similar cases that can supply at least partial information. Any problems beyond that need to be bounded.

In this case, the first step is defining an antenna model in the code that gives a good description of the real antenna. Since this is a circular polarized antenna, a means of plotting the results is developed. This is done externally to the existing code using the plotting program.

It is also desired to represent the results in absolute directive gain. This question arises frequently by users of the code. Since the NEC-BSC is not an antenna code per se. It is necessary to provide the normalizing information to the code. The surest way to obtain this information is to calculate a volumetric pattern. Integrating the volumetric pattern provides a figure for the power radiated. This number is then used to normalize the pattern. The volumetric pattern can be calculated using an ideal situation of the antenna in free space or over an infinite ground plane, which ever is more appropriate. In this case, it is an antenna over a ground plane. If one assumes that power is conserved when the model is changed, and that the current distribution does not change significantly, then this is a reasonable number to use for all the various model configurations calculated subsequently.

All the results below are shown as absolute directive gain relative to circular isotropic or linear isotropic depending on the situation.

5.3 Antenna Study

The antenna used is a Dorne & Margolin DM 1501341 (Batwing) airborne UHF satellite communication antenna. It is a circular polarized type antenna built into an aerodynamic casing. It radiates like a simple set of crossed dipoles around 16.5" in length. They are oriented parallel to the fuselage and 7.6" off of it.

One way to model an antenna in the code is to first calculate the current distribution from a method of moments code. This is done using the ESP4 code [11]. An infinite ground plane is simulated by using image elements. The results proved to be almost exactly that of using the standard dipole model in the NEC-BSC31 over an infinite ground plane. The simpler built in model is, therefore, used.

Naval Air Test Center measured the Batwing antenna on a 6 foot ground plane. The patterns are for the vertical and horizontal polarization taken at 300 MHz for various elevation cuts. Just a couple of which are shown here. The calculated and measured results for the horizontal and vertical polarized fields in the principal elevation cut of the antenna (between the two elements) is shown in Figure 5.1. The calculated and measured results for the horizontal and vertical polarized field in the elevation cut along one of the element arms is shown in Figure 5.2.

The results compare very well. If the standard model in the code had not worked out so well, then the measured result could have been used in the table look up feature of the code. The ground plane would first have to be processed out.

5.4 Model Study

Defining the model to use is the next step. The best model to use depends on the location of the antenna. Simple plan view drawings of

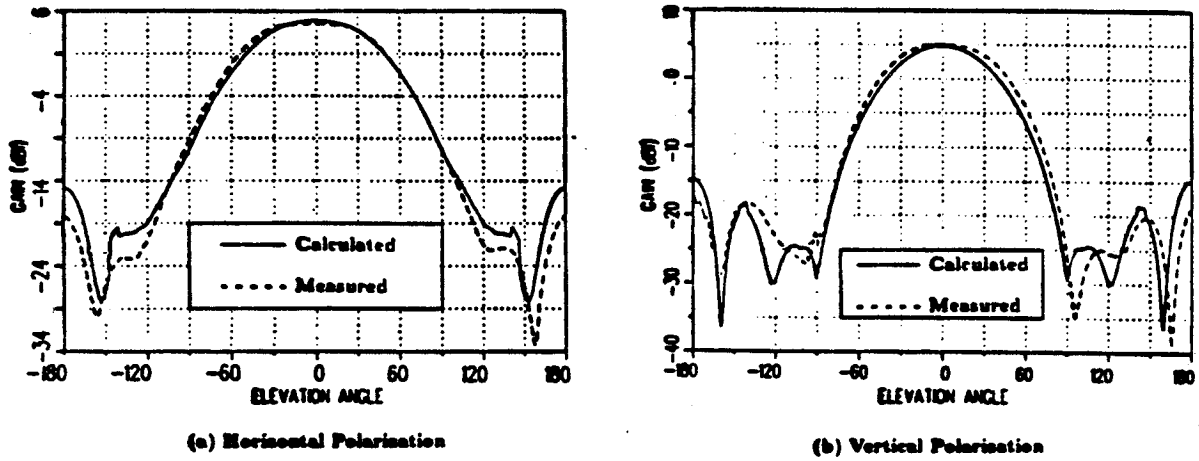

Figure 5.1: Comparison of calculated result using the NEC-BSC with measured result from NATC for horizontal and vertical polarizations of the antenna on a 6' ground plane in an elevation cut between the elements.

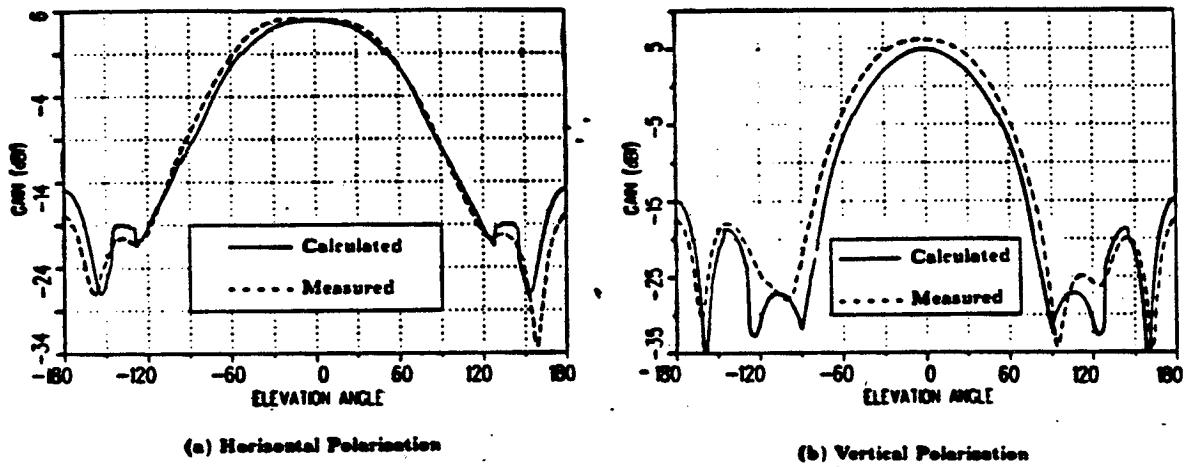

Figure 5.2: Comparison of calculated result using the NEC-BSC with measured result from NATC for horizontal and vertical polarizations of the antenna on a 6' ground plane in an elevation cut along one of the elements.

the aircraft are usually sufficient to help define the needed parameters. The measurements can be taken off the drawings then translated into the appropriate commands. The input set can then be run through the GKS geometry code, NECBSCGM, being supplied with version 3. Properly scaled this drawing can be overlaid on the plan view to see the accuracy of the input numbers.

In the case of the P-3C being studied here, any one of the three curved surface shapes can be used for the location of the antenna location used in the measurements. Figure 5.3 illustrates the use of a cylinder to represent the fuselage. An advantage of the cylinder at the present time is that the creeping waves can be calculated. For other locations closer to the nose it would be better to use on ellipsoid model. Cone frustum models are possible for other locations. In any case, it is best to start simple. Only five plates are used at first representing the wings, horizontal and vertical stabilizers.

A sensitivity study of the model is next in order. This entails running some pattern cuts with and without various parts of the structure included. If a plate representing a wing or a cylinder representing an engine does not produce significant scattering then it can be left out. It is determined by this type of analysis that the geometry in Figure 5.3 is sufficient for the indicated antenna location.

Another concern, for this particular problem, is that the antenna is only a quarter - wavelength off the surface. This pushes the largeness assumption for the UTD. This is tested by using an exact solution [12] to check the pattern in the roll plane. The dipoles are mounted on the top and oriented axially and circumferentially to an infinite cylinder in this case. The results are compared in Figure 5.4 for right and left hand polarization. This confirms that the code gives a reasonable approximation in the roll plane. Other cone angles gave similar comparisons, however, results could not be taken for very small cone angles.

The next step is to compare the patterns in the principal plane with scale model measurements. The measurements are made on a 1/17 scale model by Boeing [13]. The antenna elements are parallel to the fuselage but rotated 45° with respect to the fuselage axis. The results are compared for the roll, elevation, and azimuth planes for the right

circular component in Figures 5.5, 5.6, and 5.7, respectively. A single pattern cut took about 1.5 minutes of CPU time on a VAX 8550. Notice that the roll plane results compare excellently. The elevation and azimuth planes show deviation near the nose and tail. This is due to the interactions with the wings and stabilizers. The code does not presently have the cylinder - plate terms. These fields have been approximated by superimposing an interaction of a plate image of the antenna with the wings. On the whole, however, the comparisons are quite good over most of the patterns.

5.5 Conclusions

The NEC-BSC V3.1 has been used to predict the directive gain of a circular polarized antenna on an aircraft. The antenna model is validated against measurements on a circular ground plane. The aircraft model for a P-3C used is based on a circular cylinder fuselage with five flat plate wings and stabilizers. The model is validated by comparison with scale model measurements. The comparisons indicate that the code gives good results in most regions of the illuminate pattern. The exception is where the fuselage wing interactions have been approximated.

Numerous conic cuts have been calculated and compared with measurements with similar conclusions. Various other locations for the antenna also have been investigated. The model for the various locations are essentially the same as the one given here. When the antenna is mounted near the nose, however, a composite ellipsoidal fuselage is used. More details of this study are provided in Reference [14].

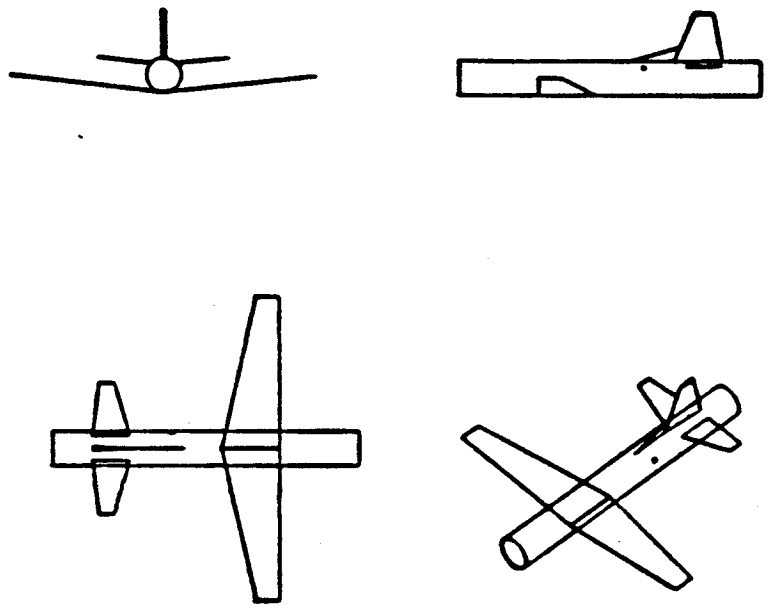

Figure 5.3: Illustration of a model of P-3C used in the NEC-BSC.

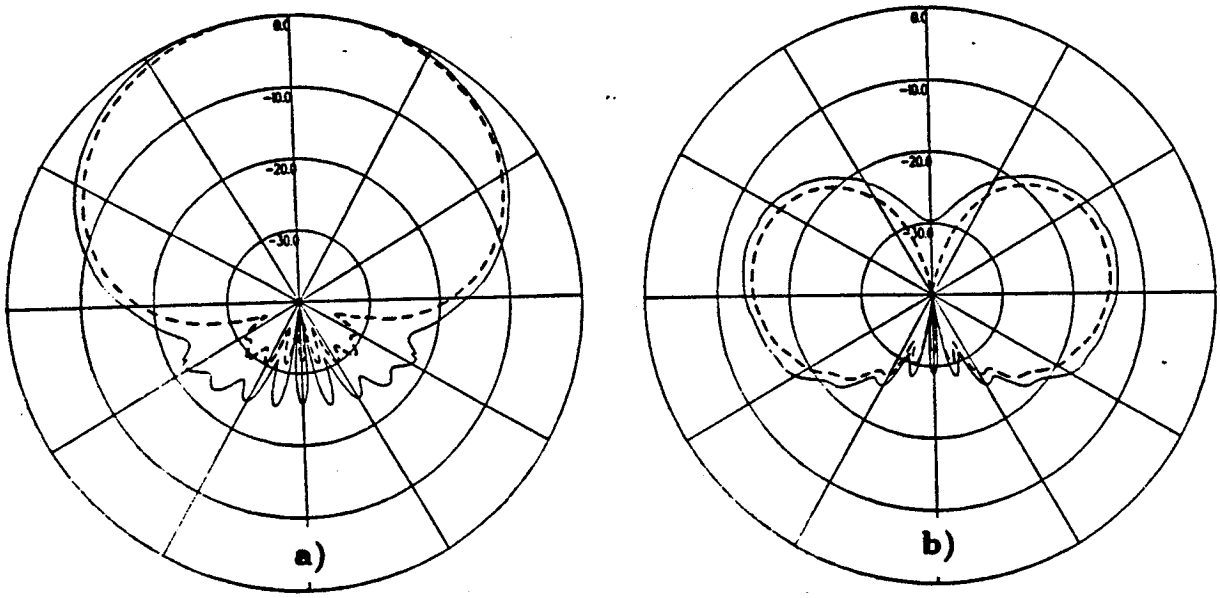

Figure 5.4: Comparison of NEC-BSC results (solid) versus an eigenfunction (dashed) solution in the roll plane of a cylinder for (a) right and (b) left circular polarization.

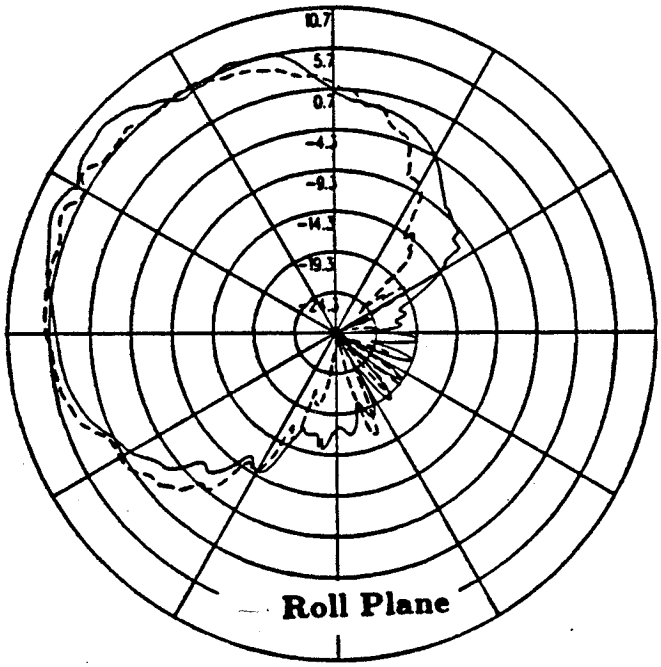

Figure 5.5: Comparison of NEC-BSC results (solid) with scale model measurements (Boeing) (dashed) for the right circular polarization in the roll plane.

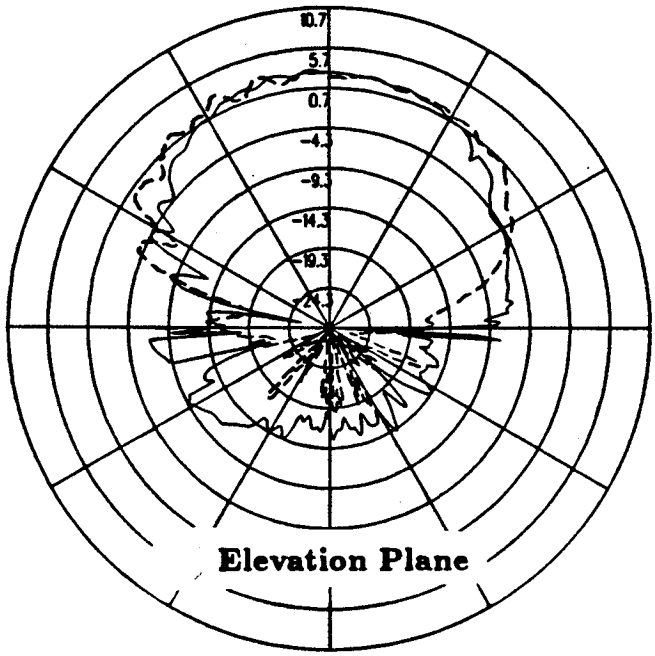

Figure 5.6: Comparison of NEC-BSC results (solid) with scale model measurements (Boeing) (dashed) for the right circular polarization in the elevation plane.

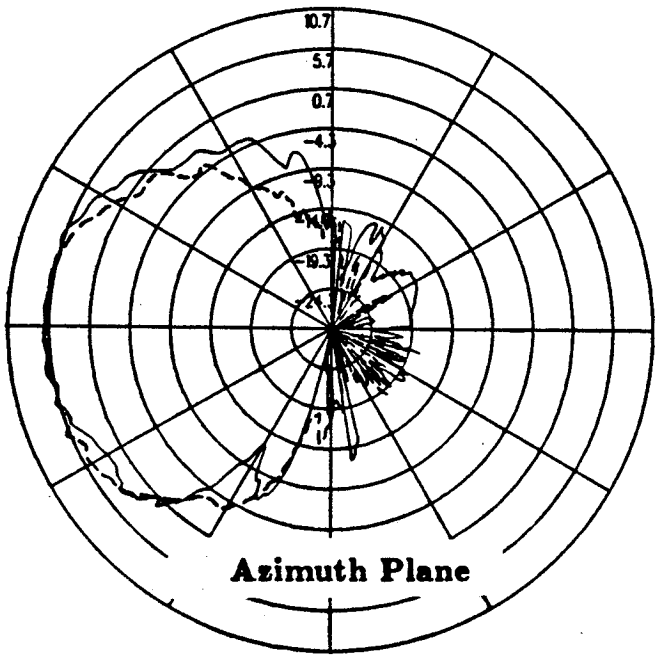

Figure 5.7: Comparison of NEC-BSC results (solid) with scale model measurements (Boeing) (dashed) for the right circular polarization in the azimuth planes

Bibliography

[1] T. Lee and W. Burnside, "Imaging processing of bistatic scattered fields obtained in a compact range," in *Proceedings of Antenna Measurement Association Techniques*, October 1989.

[2] W. D. Burnside, T. H. Lee, R. Rojas, R. J. Marhefka, and D. Bensman, "Target signature modeling and bistatic scattering measurement studies," Technical Report 721432, 721446-1, 721447-1, and 721711-1, The Ohio State University ElectroScience Laboratory, Department of Electrical Engineering, Feb. 1989. Prepared under Grant No.NAG2-542 for National Aeronautics and Space Administration Ames Research Center, Moffett Field, California.

[3] R. J. Marhefka, "Radar cross section - basic scattering code, RCS - BSC (version 2), user's manual," Technical Report 718295-15, The Ohio State University ElectroScience Laboratory, Department of Electrical Engineering, Feb. 1990. Prepared under Contract No. F33615-86-K-1023 for Wright Patterson Air Force Base.

[4] R. J. Marhefka and J. W. Silvestro, "Near zone - basic scattering code, user's manual with space station applications," Technical Report 716199-13, The Ohio State University ElectroScience Laboratory, Department of Electrical Engineering, March 1989. Prepared under Grant No. NSG 1498 for National Aeronautics and Space Administration.

[5] W. D. Burnside, J. J. Kim, B. Grandchamp, R. G. Rojas, and P. Law, "Airborne antenna radiation pattern code user's manual," Technical Report 716199-4, The Ohio State University ElectroScience Laboratory, Department of Electrical Engineer-

ing, Sep. 1985. Prepared under Grant No. NSG 1498 for National Aeronautics and Space Administration.

[6] W. F. Richards, "Microstrip antennas," in *Antenna Handbook: Theory, Applications, and Design*, (Y. T. Lo and S. W. Lee, eds.), ch. 10, New York: Van Nostrand Reinhold Co. Inc., 1988.

[7] J. J. Kim and W. D. Burnside, "Simulation and analysis of airborne antenna radiation patterns," Technical Report 716199-1, The Ohio State University ElectroScience Laboratory, Department of Electrical Engineering, Dec. 1984. Prepared under Grant No. NSG 1498 for National Aeronautics and Space Administration.

[8] R. J. Marhefka, "Development and validation of a new version of the NEC-BSC," in *4th Annual Review of Progress in Applied Computational Electromagnetics*, March 22–24 1988.

[9] P. H. Pathak, "Techniques for high-frequency problems," in *Antenna Handbook: Theory, Applications, and Design*, (Y. T. Lo and S. W. Lee, eds.), ch. 4, New York: Van Nostrand Reinhold Co. Inc., 1988.

[10] W. D. Burnside and R. J. Marhefka, "Antennas on aircraft, ships, or any large, complex environment," in *Antenna Handbook: Theory, Applications, and Design*, (Y. T. Lo and S. W. Lee, eds.), ch. 20, New York: Van Nostrand Reinhold Co. Inc., 1988.

[11] E. H. Newman and R. L. Dilsavor, "A user's manual for the electromagnetic surface patch code: ESP version III," Technical Report 716148-19, The Ohio State University ElectroScience Laboratory, Department of Electrical Engineering, May 1987. Prepared under Grant No. NSG 1613 for National Aeronautics and Space Administration.

[12] R. F. Harrington, *Time-Harmonic Electromagnetic Fields*, pp. 232–238. McGraw-Hill Book Co., 1961.

[13] S. Hunter, "P-3 update IV antenna test report," Document No. D385-66744-1, Boeing, Airborne Antenna System Group, May 1988. Prepared under Contract No. N00019-87-C-0269 for Naval Air Test Center.

[14] D. Bensman and R. J. Marhefka, "SATCOM antenna siting study on a P-3C using the NEC-BSC V3.1," Technical Report 721711-2, The Ohio State University ElectroScience Laboratory, Department of Electrical Engineering, To be published 1990. Prepared under Grant No. NAG2-542 for Naval Air Test Center and National Aeronautics and Space Administration.